Synthesis and photovoltaic application of copper (I) sulfide nanocrystals

Yue Wu[1,†] , Cyrus Wadia[1,2,†] , Wanli Ma[1], Bryce Sadtler[1], A. Paul Alivisatos[1,3,4,*]

[1]*Department of Chemistry, University of California, Berkeley, CA 94720 USA*

[2] *Energy & Resources Group, University of California, Berkeley, CA 94720 USA*

[3]*Department of Materials Science and Engineering, University of California, Berkeley, CA 94720 USA*

[4]*Materials Science Division, Lawrence Berkeley National Laboratory, Berkeley, CA 94720 USA*

† These authors contributed equally to this work

Semiconductor nanostructures are promising building blocks for future-generation photovoltaic devices, such as dye-sensitized solar cells[1-3], all-inorganic nanoparticle solar cells[4-6], and hybrid nanocrystal-polymer composite solar cells[7-10]. All of these could offer processing, scale, and cost advantages when compared with conventional single crystal and thin film solar cells. One of the most challenging aspects in this area is to find a semiconductor material with a suitable band gap, near 1 eV for a conventional, single-gap device, which can be made in nanostructured form, using earth-abundant elements, and of environmentally benign composition. Here we explore a candidate material satisfying these requirements: copper (I) sulfide, Cu_2S. We present a synthesis of colloidal copper sulfide nanocrystals. As a first example of utilization in a solar cell, we demonstrate their utilization as an active light absorbing component in

combination with CdS nanorods to make a solution-processed solar cell with 1.6% power conversion efficiency and stability over a 4 months testing period.

Cu_2S is an indirect gap semiconductor with a bulk bandgap of 1.21 eV[11]. Its use in combination with CdS as a solar cell material was extensively investigated from 1960s to the 1980s[12-17]. In thin film studies, Cu_2S/CdS solar cells did show significant promise, but copper diffusion into and doping of the CdS layer led to long-term performance degradation and ultimately abandonment of this system. With the advent of nanocrystal-based approaches which can use much milder processing conditions, and in which diffusion and doping issues take on entirely new character, it is well worthwhile to re-examine this material combination. CdS nanocrystals are of course widely available and can be synthesized with exquisite control over size, shape, and new processing approaches[18-20]. In contrast, there are only a few reports of Cu_2S nanocrystal synthesis[21-23].

Our synthesis of colloidal Cu_2S nanocrystals involves an injection reaction between copper (II) acetylacetonate and ammonium diethyldithiocarbamate in a mixed solvent of dodecanethiol and oleic acid (see Methods). X-ray diffraction (XRD) studies (Fig. 1a) show the materials prepared in this way are hexagonal chalcocite Cu_2S (JCPDS 026-1116, Fig. 1a red lines). Low-resolution transmission electron microscopy (TEM) studies (Fig. 1b) show nanocrystals with an average size of 5.4 ± 0.4 nm. High-resolution TEM studies (upper inset, Fig. 1b) confirm that the observed nanocrystals are Cu_2S and show several important features. First, the TEM data demonstrate clearly that the Cu_2S nanocrystals are single crystal structures. Second, these Cu_2S nanocrystals have a well-defined hexagonal-faceted structure (dashed line, upper inset, Fig. 1b). Third, the reciprocal lattice peaks, which were obtained from two-dimensional Fourier transforms (2DFT) of the lattice-resolved image (low inset, Fig. 1b) can be indexed to the hexagonal structure of Cu_2S with the zone axes along the $[1\bar{2}1\bar{3}]$ direction.

The optical properties of the Cu_2S nanocrystals have been studied by UV-Visible (UV-Vis.) absorption spectroscopy and photoluminescence (PL) to further assess their quality. A representative UV-Vis. spectrum (Fig. 1c, see Methods) recorded from Cu_2S nanocrystals dispersed in chloroform at room temperature shows a wide absorption up to ca. 1000 nm. Lastly, PL studies (inset, Fig. 1c, see Methods) show a single peak centered at 1.26 eV, which is similar with reported bulk value of 1.21 eV[11], with a full-width at half maximum (FWHM) of 0.19 eV.

The single crystal Cu_2S nanocrystals have potential photovoltaic application, and we have explored this possibility. We prepared solar cell devices through a low temperature (≤150 °C) solution process in which the critical heterojunction is formed between a layer of spin-cast Cu_2S nanocrystals and a layer of spin-cast CdS nanorods (Fig. 2a, see Methods). The thickness of the Cu_2S nanocrystal layer and the CdS nanorod layer are measured to be around 300 nm and 100 nm, respectively, with total film surface roughness to be less than 4 nm (inset, Fig. 2b) and an average optical density of 1.1.

Representative current density (*J*)-voltage (*V*) characteristics recorded on the as-made photovoltaic device show typical rectification behaviour under zero illumination (black curve, Fig. 3a). Under a standard illumination (irradiance 100 mW/cm^2, temperature 25°C, AM = 1.5G), the device shows an open circuit voltage (V_{oc}) of 0.6 V and a short circuit current density (J_{sc}) of 5.63 mA/cm^2 (red curve, Fig. 3a), corresponding to a power conversion efficiency (η) of 1.6% with a fill factor (FF) of 0.474. Spectral response measurements (Fig. 3b) show external quantum efficiencies (EQE) approaching 40% in the device (see Methods). Integration of the obtained external quantum efficiency data with the true AM1.5G solar emission spectrum matches well with the short-circuit currents obtained under simulated AM1.5G illumination (Fig. 3a).

Analysis of these results highlights some important points. First, V_{oc} for our Cu_2S-CdS nanocrystal-based solar cell is better than the best values, 0.54 V[12], reported for the conventional Cu_2S-CdS thin film solar cells that were widely studied between the 1960s and1980s[12-17]. This may be due to the planar junction between Cu_2S and CdS generated during sequential spin coating (total roughness ~ 4 nm), avoiding the textured junction generated in the 'wet' (dipping CdS into CuCl aqueous solution) or 'dry' process (formation of Cu_2S by evaporating CuCl on CdS followed by annealing)[16]. Furthermore, the performance of the devices is reproducibly achieved without large energy input for high temperature annealing or sintering, which gives our devices a distinct advantage over previous all-inorganic nanocrystal photovoltaic devices[4].

Two unusual features which were well studied in the thin film CdS-Cu_2S solar cells are also observed in the system we have prepared. First, the *I-V* curves measured in the light and dark intersect (Fig. 3a). Such behaviour was also observed in annealed CdS-Cu_2S thin film cells and labelled as the cross-over effect[14, 16, 17]. The second unusual effect is that the action spectrum for the solar cells shows a threshold energy that is greater than the band gap of the Cu_2S. There is no photocurrent generated for photons to the red of 700 nm, even though the Cu_2S continues to absorb as far red as 800 nm, and the band offsets of the native components are such that all photogenerated electrons should flow readily to the CdS, and holes to the Cu_2S.

Both effects can be traced to the development of an energetic barrier for electrons in an interfacial zone between the Cu2S and CdS layers[14, 15]. This spike or barrier in the electron potential arises when Cu ions diffuse a short way into the CdS layer. Photogenerated electrons must have enough energy to overcome this barrier. Further, the crossover effect in the I-V curve arises again because photoexcited electrons with sufficient energy can overcome this barrier.

The photovoltaic parameters have also been determined as a function of illumination intensity (I). The experimental data (black dots, Fig. 3c) show a near-linear relationship (red curve, Fig. 3c) between the light intensity and the short circuit current density: $J_{sc} \propto I^n$, with n = 0.97. The near-linear relationship implies only minor charge-carrier recombination is occurring in these photovoltaic devices[25]. Furthermore, during a four months measurement period, an encapsulated device shows a nearly constant performance (Fig. 3d). This is in contrast to other thin film studies which typically showed degradation in shorter time intervals, due to facile Cu diffusion. It may be that in our devices, there is a network of necked nanocrystals, and the diffusion of copper through this network is retarded compared to the diffusion in conventional thin films. There is some evidence that a fraction of the dodecane thiol capping ligands survive the film deposition steps (unpublished result), potentially passivating some trap sites and also serving as barrier layers to retard ion diffusion[24].

Lastly, the ability to fabricate functional nanocrystal solar cells through a simple low temperature solution process suggests the possibility of transferring this technique onto plastic substrates, which could offer many attractive properties including flexibility, light weight, shock resistance, softness, and transparency[26-28]. As a demonstration, we fabricated Cu_2S-CdS solar cells on an ITO-coated plastic substrate (upper inset, Fig 4. see Methods). The device shows a similar performance to the ones fabricated on conventional ITO glass substrate (red curve, Fig. 4. V_{oc} = 0.574 V, J_{sc} = 5.625 mA/cm^2, FF = 0.494, η = 1.604%). In addition, we have investigated the behaviour of the nanocrystal solar cell device on the plastic substrate after bending. A comparison of performance recorded when the device was originally flat (red curve, Fig. 4) versus released to flat after bent to a curvature of 105° (green curve, Fig. 4) shows that there is only a small change after the bending. There is a slight decrease in open circuit voltage (V_{oc} = 0.552 V) and a slight increase in short circuit current (J_{sc} = 6.050 mA/cm^2) for the device after the bending, corresponding to an overall decrease of power efficiency to

1.472%. This change is small (~ 8%) given the large stress on the device during the bending and clearly shows the robust nature of our nanocrystal/plastic solar cells and the potential as the power source for flexible handheld consumer electronics.

In summary, our studies show that narrow size distribution single crystal Cu_2S nanocrystals can be synthesized in a solution-phase reaction. The incorporation of the Cu_2S nanocrystals into photovoltaic devices yields a power conversion efficiency exceeding 1.6%. Furthermore, the low temperature solution-phase process used to fabricate these nanocrystal solar cell devices opens up the possibility of a promising technique for low-cost power conversion on plastic substrates for future flexible electronics. While the CdS in our device does pose toxicological concerns, Cu_2S, in principle, can be paired with other earth abundant and non-toxic semiconductors to form new sets of photovoltaic materials, which makes the present work a necessary and important intermediate step towards the discovery of these potential systems.

Methods

Preparation and characterization of single-crystal Cu_2S nanocrystals and CdS nanorods for photovoltaic devices

All chemicals are purchased from Aldrich, and used without any further purification. In a typical synthesis of Cu_2S nanocrystals, 1.25 mmol of ammonium diethyldithiocarbamate is mixed with 10 mL dodecanethiol and 17 mL oleic acid in a three-neck flask. The solution is heated up to 110 °C under Argon (Ar) flow followed by a quick injection of a suspension composed of 1 mmol copper (II) acetylacetonate and 3 mL oleic acid. Then, the solution is quickly heated up to 180 °C and kept at the temperature for 10-20 minutes.

The cleaning of the nanocrystals involves multiple steps performed in a glovebox with Ar protection and all the solvents used are anhydrous to avoid any possible oxidation. Right after the reaction, the solution containing Cu_2S nanocrystals is cooled down naturally to 120 °C before taken out of flask for centrifuging at 4600 rpm for 10 minutes. The supernatant is discarded and the precipitation is first fully dissolved in 4 g of toluene and then precipitated out by adding11g of isopropanol followed by centrifuging at 4600 rpm for 10 minutes. This procedure is repeated three times to clean away the residue of dodecanethiol and oleic acid. The synthesis of the CdS nanorods is conducted in a similar manner mention above and the exact details can be found in Ref. 18.

After that, the Cu_2S nanocrystals and the CdS nanorods are dissolved separately into 15 mL pyridine and kept at 120 °C for at least one day, allowing for comprehensive ligand exchange, followed by precipitated out using appropriate amount of hexane. The Cu_2S nanocrystals and the CdS nanorods are then dissolved separately into appropriate amount of chloroform ($CHCl_3$) and then passed through a 0.4 μm Teflon filter to make stock solutions for photovoltaic device fabrication.

Fabrication and characterization of Cu_2S-CdS nanocrystal photovoltaic devices

Glass substrates coated with 150 nm ITO (Thin Film Devices Inc., resistivity 20 ohms/sq) are cleaned by ultrasonication for ca. 30 minutes in an even mixture of acetone and isopropanol and then deionized water, respectively. The substrates are then dried under a stream of nitrogen followed by oxygen plasma cleaning for 15 minutes at 0.2 torr. A filtered dispersion of PEDOT:PSS in water (Baytron-PH) was immediately spin-cast at 4000 rpm for one minute and then baked for 30 minutes at 120 °C. After cooling down, nanocrystal films are spin-cast at 600 rpm onto the substrates. To create bilayer structures, Cu_2S films are spin-cast first and then heated for 10 minutes at 150 °C to remove excess solvent and allow for spin-casting of the second films of CdS.

Then, the substrates are annealed again for 5~10 minutes at 150 °C. After that, the substrates are held at ca. 10^{-7} torr for up to 12 hours, after which 200 nm of top aluminum (Al) electrodes are deposited by thermal evaporation through a shadow mask, resulting in individual devices with 0.04 cm^2 nominal areas. After evaporation, a rapid thermal annealing is performed on the devices at 150 °C for 30~60 seconds. The procedure of fabricating photovoltaic device on plastic substrate is same as above except ITO-coated plastic substrates (OC50, CP Films) are used to replace the regular ITO-coated glass substrates. Accordingly, the oxygen plasma cleaning time is reduced to 3.5 minutes.

Simulated AM1.5G illumination is obtained with a Spectra Physics Oriel 300W Solar Simulator with AM1.5G filter set. The integrated intensity is set to 100 mW/cm^2 using a thermopile radiant power meter (Spectra Physics Oriel, model 70260) with fused silica window, and verified with a Hamamatsu S1787-04 diode. Intensity is controlled to be constant throughout measurements with a digital exposure controller (Spectra Physics Oriel, model 68950).

References

1. Law, M., Greene, L. E., Johnson, J. C., Saykally, R., Yang, P. D., Nanowire dye sensitized solar cells. *Nature Mater.* **4**, 455-459 (2005).

2. Grätzel, M. Conversion of sunlight to electric power by nanocrystalline dye-sensitized solar cells. *J. Photoch. Photobio. A.* 164, 3-14 (2004).

3. Baxter, J. B., Aydil, E. S. Nanowire-based dye-sensitized solar cells. *Appl. Phys. Lett.* **86**, 053114 (2005).

4. Gur, I., Fromer, N. A., Geier, M. L., Alivisatos, A. P. Air-stable all-inorganic nanocrystal solar cells processed from solution. *Science* **310**, 462-465 (2005).

5. Leschkies, K. S., Divakar, R., Basu, J., Enache-Pommer, E., Boercker, J. E., Carter, C. B., Kortshagen, U. R., Norris, D. J., Aydil, E. S. Photosensitization of ZnO nanowires with CdSe quantum dots for photovoltaic devices. *Nano Lett.* **7**, 1793-1798 (2007).

6. Tian, B., Zheng, X., Kempa, T. J., Fang, Y., Yu, N., Yu, G., Huang, J., Lieber, C. M. Coaxial silicon nanowires as solar cells and nanoelectronic power sources. *Nature* **449**, 885-889 (2007).

7. Huynh, W. U., Dittmer, J. J., Alivisatos, A. P. Hybrid nanorod-polymer solar cells. *Science* **295**, 2425-2427 (2002).

8. Gur, I., Fromer, N. A., Chen, C., Kanaras, A. G., Alivisatos, A. P. Hybrid solar cells with prescribed nanoscale morphologies based on hyperbranched semiconductor nanocrystals. *Nano Lett.* **7**, 409-414 (2007).

9. Cui, D. H., Xu, J., Zhu, T., Paradee, G., Ashok, S., Gerhold, M. Harvest of near infrared light in PbSe nanocrystal-polymer hybrid photovoltaic cells. *Appl. Phys. Lett.* **88**, 183111 (2006).

10. Beek, W. J. E., Wienk, M. M., Janssen, R. A. J. Efficient hybrid solar cells from zinc oxide nanoparticles and a conjugated polymer. *Adv. Mater.* **16**, 1009-1013 (2004).

11. Liu, G., Schulmeyer, T., Brötz, J., Klein, A., Jaegermann, W. Interface properties and band alignment of Cu_2S/CdS thin film solar cells. *Thin Solid Films* **431-432,** 477–482 (2003).

12. Rothwarf, A., Barnett, A. M. Design analysis of the thin-film CdS-Cu_2S solar cell. *IEEE T. Electron Dev.* 24， 381-387 (1977).

13. Böer, K. W. The CdS/Cu_2S solar cell. *J. Crystal Growth* **59**, 111-120 (1982).

14. Gill, W. D., Bube, R. H. Photovoltaic Properties of Cu_2S-CdS heterojunctions. *J. Appl. Phys.* **41**, 3731-3738 (1970).

15. Fahrenbr, A. L., Bube, R. H. Heat-treatment effects in Cu_2S-CdS heterojunction photovoltaic cells. *J. Appl. Phys.* **45**, 1264-1275 (1974).

16. Pfisterer, F., The wet-topotaxial process of junction formation and surface treatments of Cu_2S-CdS thin-film solar cells. *Thin Solid Films* **431**, 470-476 (2003).

17. Rothwarf, A. The CdS-Cu_2S solar cell: basic operation and anomalous effects. *Solar Cells* **2**, 115-140 (1980).

18. Yong, K., Sahoo, Y., Swihart, M. T., Prasad, P. N. Shape control of CdS nanocrystals in one-pot synthesis. *J. Phys. Chem. C* **111**, 2447-2458 (2007).

19. Li, Y., Liao, H., Ding, Y., Qian, Y., Yang, L., Zhou, G. Nonaqueous synthesis of CdS nanorod semiconductor. *Chem. Mater.* **10**, 2301-2303 (1998).

20. Peng, Z. A., Peng, X. Formation of High-Quality CdTe, CdSe, and CdS Nanocrystals Using CdO as Precursor. *J. Am. Chem. Soc.* **123**, 183-184 (2001).

21. Sigman, M. B., Ghezelbash, A., Hanrath, T., Saunders, A. E., Lee, F., Korgel, B. A. Solventless synthesis of monodisperse Cu2S nanorods, nanodisks, and nanoplatelets. **125**, 16050-16057 (2003).

22. Brelle, M. C., Torres-Martinez, C. L., McNulty, J. C., Mehra, R. K., Zhang, J. Z. Synthesis and characterization of Cu_xS nanoparticles. Nature of the infrared band and charge-carrier dynamics. *Pure Appl. Chem.* **72**, 101-117 (2000).

23. Ghezelbash, A., Korgel, B. A. Nickel sulfide and copper sulfide nanocrystal synthesis and polymorphism. *Langmuir* **21**, 9451-9456 (2005).

24. Yang, H., Holloway, P. H. Enhanced photoluminescence from CdS:Mn/ZnS core/shell quantum dots. *Appl. Phys. Lett.* **82**, 1965-1967 (2003).

25. Nelson, J. Diffusion-limited recombination in polymer-fullerene blends and its influence on photocurrent collection. *Phys. Rev. B* **67**, 155209 (2003).

26. Mcalpine, M. C., Friedman, R. S., Lieber, C. M. High-performance nanowire electronics and photonics and nanoscale patterning on flexible plastic substrates. *P. IEEE* **93**, 1357-1363 (2005).

27. McAlpine, M. C., Ahmad, H., Wang, D., Heath, J. R. Highly ordered nanowire arrays on plastic substrates for ultrasensitive flexible chemical sensors. *Nature Mater.* **6**, 379-384 (2007).

28. Sun, Y., Rogers, J. A. Inorganic semiconductors for flexible electronics. *Adv. Mater.* **19**, 1897-1916 (2007).

Acknowledgements. We thank Steven Hughes, Jungwon Park, Ching Ting, Jonathan S. Owen, and Paul-Emile Trudeau for helpful discussions. Yue Wu thanks the Miller Institute for Basic Research in Science for Miller Research Fellowship. Cyrus Wadia thanks the Environmental Protection Agency for the EPA STAR Fellowship. This work was supported by DAF AFOSR under award No. FA9550-06-1-0488 and

the Director, Office of Science, Office of Basics Energy Sciences, Materials Sciences and Engineering Division, of the U. S. Department of Energy under Contract No. DE-AC02-05CH11231.

Competing interests statement. The authors declare that they have no competing financial interests.

Correspondence and requests for materials should be addressed to A. P. A. (e-mail: alivis@berkeley.edu.).

Figure Captions

Figure 1 Structural characterization of Cu_2S nanocrystals. **a,** XRD diffraction pattern of Cu_2S nanocrystals, which can be indexed to hexagonal Cu_2S (JCPDS 026-1116, red lines). **b,** TEM image of Cu_2S nanocrystals with an average diameter of ca. 5.4 nm. The scale bar is 10 nm. Upper inset, high magnification TEM image of Cu_2S nanocrystal shows single crystal hexagonal faceted structure. The scale bar is 1 nm. Lower inset, 2DFT of the image showing the $[1\bar{2}1\bar{3}]$ zone axis of Cu_2S. **c,** UV-Vis. absorption spectrum of Cu_2S nanocrystals shows a wide absorption up to ca. 1000 nm. Inset, PL spectrum shows a single peak centered at 1.26 eV.

Figure 2 Fabrication and characterization of Cu_2S-CdS nanocrystals photovoltaic devices. **a,** Scheme of Cu_2S-CdS nanocrystals photovoltaic device fabrication. (1) Solution-phase synthesises of Cu_2S nanocrystals and CdS nanorods. (2) Cu_2S nanocrystals and CdS nanorods are cleaned to make stock solutions for photovoltaic device fabrication. Inset, TEM image of CdS nanorods. The scale bar is 50 nm. (3) PEDOT:PSS, Cu_2S nanocrystals and CdS nanorods.are sequentially spin-cast onto ITO-coated glass substrates. (4) Al electrodes are thermally evaporated onto the substrates under high vacuum and electrical measurements are performed. Inset, photography of the Cu_2S-CdS nanocrystals photovoltaic device. **b,** UV-Vis spectra of ITO-coated glass substrate (black curve), ITO substrate with PEDOT:PSS layer (red curve), ITO substrate with PEDOT:PSS and Cu_2S layers (green curve), and final device (ITO substrate with PEDOT:PSS, Cu_2S, and CdS layers, blue curve). Inset, AFM image of the final device shows an overall roughness less than 4 nm.

Figure 3 Electrical measurements of Cu_2S-CdS nanocrystals photovoltaic devices. **a,** Current density-voltage characteristics of the photovoltaic device

under zero illumination (black curve) and standard illumination (red curve, irradiance 100 mW/cm^2, temperature 25°C, AM = 1.5G) showing a power conversion efficiency of 1.600%. Inset, band alignment of Cu_2S-CdS. **b,** Spectral response measurement showing the external quantum efficiencies approaching 40%. **c**, Short circuit current density J_{sc} vs. illumination intensity I (black dots) show shows a near-linear relationship to a (red curve, $J_{sc} \propto I^n$, with n = 0.97). **d**, Life time measurement over 60 days shows no significant degradation in efficiency.

Figure 4 Cu_2S-CdS nanocrystals photovoltaic devices on plastic substrate. Current density-voltage characteristics of the photovoltaic device under zero illumination (black curve) and standard illumination when flat (red curve, 1.604% power conversion efficiency) and released to flat after bent to a curvature of 105°(green curve, 1.472% power conversion efficiency). The decrease in efficiency due to the bending is small (~8%) given the large stress on the device during the bending and clearly shows the robust nature of our nanocrystal/plastic solar cells. Shown in the inset is a photograph of the Cu_2S-CdS nanocrystals plastic solar cells.

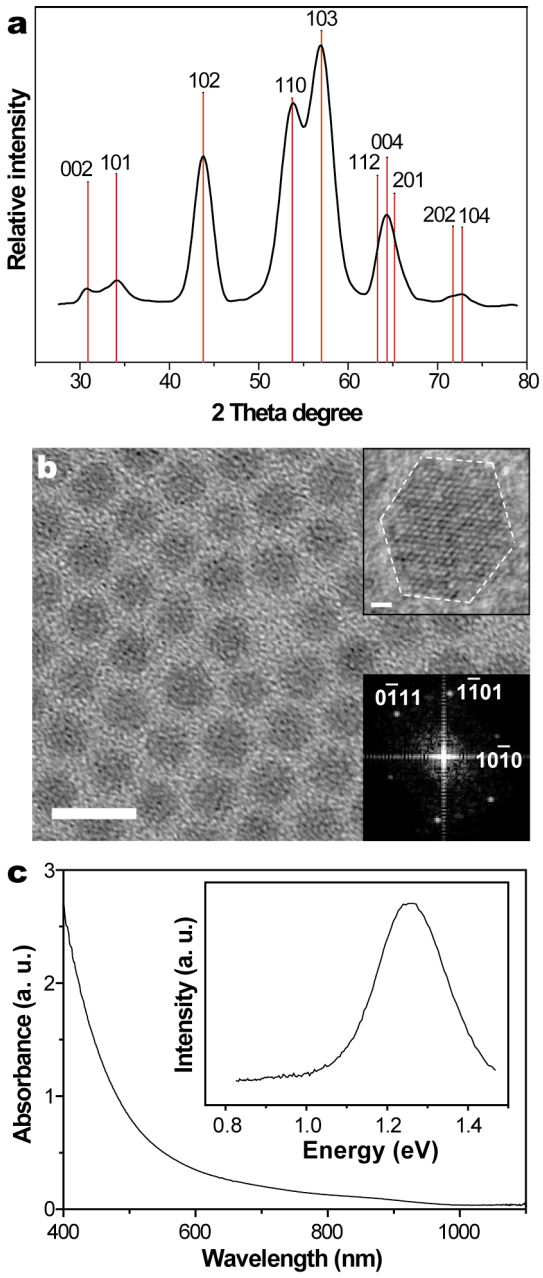
a
Relative intensity
002
101
102
110
103
112
004
201
202
104
30
40
50
60
70
80
2 Theta degree
b
$0\bar{1}11$
$1\bar{1}01$
$10\bar{1}0$
c
Absorbance (a. u.)
0
1
2
3
400
600
800
1000
Wavelength (nm)
Intensity (a. u.)
0.8
1.0
1.2
1.4
Energy (eV)

Figure 1

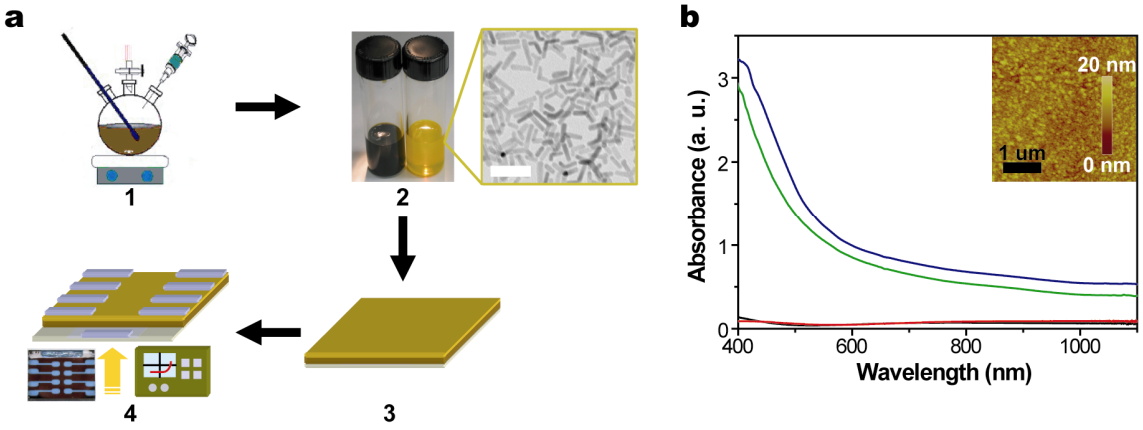

Figure 2

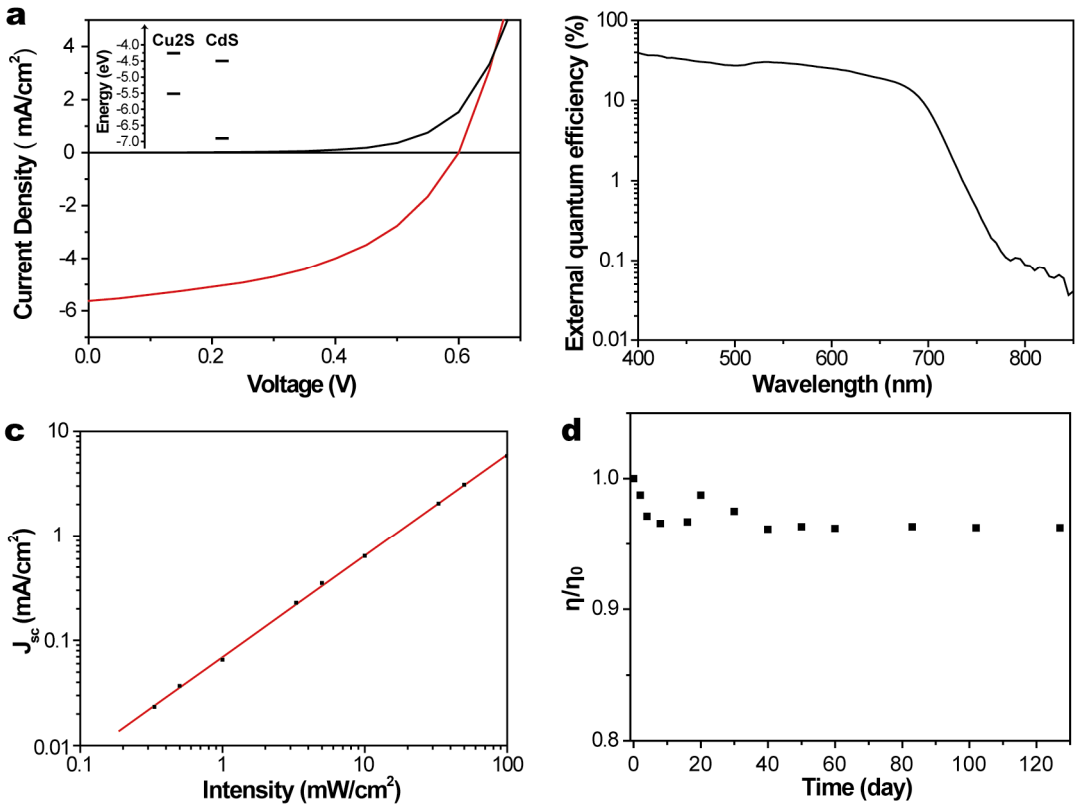

Figure 3

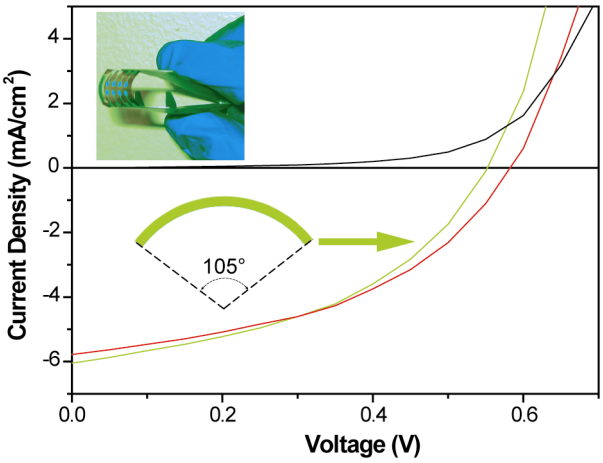

Figure 4

DISCLAIMER